Cement and Concrete Research xxx (2016) xxx–xxx

Contents lists available at ScienceDirect

Cement and Concrete Research

journal homepage: www.elsevier.com/locate/cemconres

Numerical modelling of porous cement-based materials by superabsorbent polymers

Ismael Viejo[a,*], Luis Pedro Esteves[b], Manuel Laspalas[a], José Manuel Bielsa[a]

[a] ITAinnova - Instituto Tecnológico de Aragón, María de Luna 8, Zaragoza 50018, Spain
[b] Department of Civil Engineering, Technical University of Denmark, Building 118, Brovej, Lyngby DK-2800, Denmark

ARTICLE INFO

Article history:
Received 1 December 2015
Received in revised form 6 July 2016
Accepted 28 July 2016
Available online xxxx

Keywords:
SAP
FE micromechanics
Continuum micromechanical

ABSTRACT

The development of new cementitious materials raises new challenges with regard to structural design. One of the potential applications of superabsorbent polymers (SAP) is to deliver well-defined porosity to cement systems. This is particularly interesting for the development of porous cement-based materials with high technical performance. In this paper, a numerical approach to model the basic mechanical properties of the porous cement with SAP is developed. The modelling approach is based on computational micromechanics and uses a representative volume element that emulates the microstructure of the cement-based material to determine the overall material response and the local behaviour. Using this approach several sensitivity analyses are undertaken examining various parameters. The modelling approach is compared with experimental results showing reasonable correlation. The proposed approach provides faster and cheaper tool to design porous materials due to a reduction in the required experimental effort.

1. Introduction

The design of porous cement-based materials establishes a challenge to obtain light materials while maintaining high technical performance. Superabsorbent polymers (SAP) can bring great flexibility to the design of porous cement-based materials, allowing to tailor the pore structures thanks to a basic knowledge of the absorbency of the polymer. The specific morphology of the resultant pores has a high potential of improving the mechanical performance of low density cement-based materials.

Nevertheless, the design of these materials, as with other composite materials, requires a costly experimental development plan in order to establish the dosages that will provide the required material properties. In this process, the use of micromechanical models can complement the experimental tasks predicting the final properties of the heterogeneous material, thus reducing the required experimental effort in favour of the development of the material.

Continuum micromechanical models offer a framework to analyse the behaviour of heterogeneous materials. The underlying idea behind continuum micromechanics is that it is possible to separate a heterogeneous material into phases with on-average constant material properties. According to this concept, the main goal of micromechanics is predicting the response of a heterogeneous material on the basis of the geometries, volume fractions and properties of the individual phases (homogenisation). These models can be roughly classified as analytical or numerical (computational). From a theoretical perspective, analytical micromechanical models are based on important assumptions and simplifications that limit their applicability to simple material systems. Other analytical approaches are based on mathematical regressions over empirical data, therefore having a less meaningful physical background.

In order to overcome part of these limitations, the computational approaches are feasible alternative tools to be used in the design of composite materials. They allow to analyse more complex morphologies and to model non-linear constituents behaviour while providing a simpler way to account for localized deformation and failure mechanisms [1].

One of the most commonly used computational approaches is based on the Finite Element Method (FEM), where a representative volume element (RVE) is built reproducing the morphology of the constituents and the appropriate material models assigned to each phase [2–5] . The prediction of the homogenised material behaviour is obtained subjecting this RVE to a load state, normally under pure uniaxial tensile or compression load or shear load. The

* Corresponding author.
E-mail address: iviejo@itainnova.es (I. Viejo).

http://dx.doi.org/10.1016/j.cemconres.2016.07.018
0008-8846/

accuracy of this prediction will depend on the exactitude of the modelled morphology, material model considered for each constituent, boundary conditions and mesh size.

Analytical and numerical micromechanical models have been applied to the prediction of the effective properties of different types of composites (mainly metallic and plastic composites), including cement-based materials as described below.

The use of analytical methods is focused on the estimation of linear effective properties, such as elastic modulus, several of these contributions are summarized hereinafter. Bary [6] compares the prediction obtained with the Mori-Tanaka (M-T), Self-consistent (S-C) and Interaction Direct Derivate (IDD) schemes and a numerical approach by means of FEM. Šmilauer [7] also compares the prediction of the M-T scheme and FEM. Bernard [4] combines the S-C and M-T schemes in order to predict the elastic modulus at early stages of paste hydratation and its evolution over time. Sorelli [8] utilizes an M-T scheme at every phase. Hernández [9] and Acebes [10] propose the formulation of a three-phase model based on a mean field theory of M-T and Eshelby's equivalent inclusion principle, estimating some mechanical properties in n-phases cement composite.

In addition to previous contributions, mainly focused on using analytical models, several papers have employed numerical approaches for cement-based materials, modelling factors from elastic properties to the damage mechanisms. Most of the papers use FEM to predict the elastic behaviour of the material by volumetric averaging from the elastic moduli of the individual phase, as in Kamali [11], Haecker [12], Šmilauer [7] or Toulemonde [13]. Other authors have analysed more complex phenomena, including crack generation or damage distribution. Bernard [1] studied the mechanical behaviour at the mortar level, obtaining the crack pattern under tensile and compression loads by using a Rankine criteria for the maximal principal stress. Kim [14] analysed concrete behaviour of a 3-phase composite material mortar, aggregates and interface by a simulation based on a coupled plasticity-damage model.

While there are numerous papers focused on the study of cement materials by means of continuum micromechanics, the study of porous cement-based materials is not common in literature. Furthermore, the prediction of compression or tensile strength using these models is also unusual. In that area, Yaman [15] utilized several semi-empirical models for the prediction of the elastic modulus as function of the porosity while Gibson [16] defined an equation for closed-cell foams in general. Additionally, there are other empirical models that define the link between the compression strength and the porosity such as the Balshin's model, Powers' gel-space ratio equation or others based on previous ideas [17].

In the present study, a methodology to predict the behaviour of a porous cement-based material is described. The methodology used is based on continuum micromechanics using FEM to evaluate the RVE of the porous cement. The effective and local behaviour of this material (elastic modulus and strengths) is analysed under uniaxial deformation. The validation of this approach for a porous cement-based material is carried out through comparison with experimental data. Finally, using this numerical tool, the influence of different morphological and material properties is studied through sensitivity analyses.

Following this introduction and review of the state of the art, the paper comprises an initial section describing the characteristics of the material system object of the study and the performed experimental characterization tests. The numerical methodology is fully described in the subsequent section, including RVE generation, boundary conditions, material model and prediction procedure. This is followed by a comparison between the numerical prediction and the characterized porous material. Results are discussed in the next section, which continues with several sensitivity analyses undertaken using the developed methodology. The study ends with a set of conclusions.

2. Porous cement-based materials by superabsorbent polymers

Porous cement-based materials consist of a pore agent and a solid cementitious skeleton. The basic principles to design cement with a variety of pore agents are described by Esteves [18].

In the design of porous cement-based materials with SAP, the definition of the water entrained particle-based system in the material is critical because it determines the porosity in its hardened state. The measurement of this water entrained is performed by an absorbency measurement based on the principle of laser diffraction particle size analysis [19]. The measurement of the relevant SAP provides to an absorbency of 20 ml/g. The material design was performed using SAP with a dry mode of 100 μm, that is, the mean diameter of SAP particles without added water is 100 μm, which leads to a swollen mode size of about 300 μm. The particle size distribution (PSD) of the porosity added by SAP at the hardened cement is obtained by measurement of PSD of the swollen SAP using the laser diffraction technique particle [19], assuming that the PSD measured in the relevant cementitious environment defines a stable swollen state during the setting and hardening of cement. This value is confirmed by computerized tomography of the relevant materials. The generated microstructure can be observed in Fig. 1.

The experimental methods included the determination of the modulus of elasticity in compression, compressive and flexural strength, density and air content of the material. Standard methods were used for this experimental setup. The densities of both fresh and hardened materials were calculated in accordance with EN 12390-7:2009, by measuring the mass and volume of the specimens. Since the systems are sealed cured, the hardened density can be considered identical to the fresh density of the material. This fact was supported by mass measurements before and after sealed curing. The method for the determination of air content followed the procedure described in EN 12350-7:2009 - the pressure gauge method. The cementitious system, enclosing an unknown amount of air, is subjected to a known pressure by introducing a certain volume of air. The dial on the pressure gauge is calibrated in terms of percentage of air for the resulting pressure. The procedure for stress-strain relationship determination included the use of linear transducers

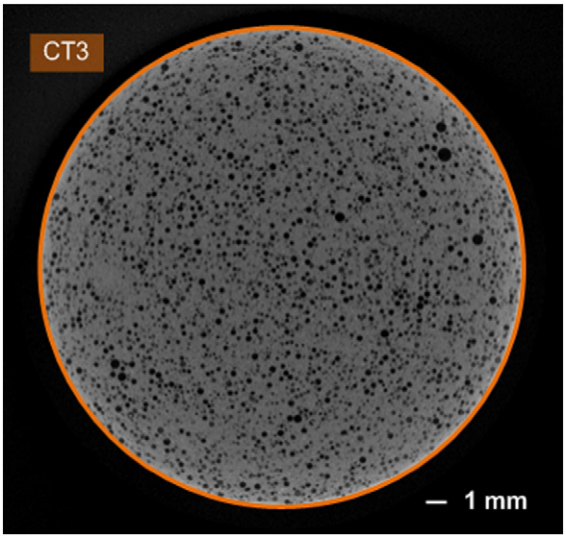

Fig. 1. Microstructure of porous cement-based materials with SAP. The cement paste is composed of cement and water at a w/c ratio of 0.25 by mass. SAP was added at a rate of 0.5% by cement mass. This corresponds to a total porosity value of about 40%. The image shows a computerized tomography scanned slice, where grey colour is the cement paste and black colour are holes corresponds with porosity mainly associated to SAP due to the higher scale.

Please cite this article as: I. Viejo et al., Numerical modelling of porous cement-based materials by superabsorbent polymers, Cement and Concrete Research (2016), http://dx.doi.org/10.1016/j.cemconres.2016.07.018

physically attached to the sample in two positions opposite to each other. No stabilizer was used, so partly-rotation of the fixtures was possible. The results are based on the average of two transducers. Stress-strain in compression was measured to 50% of the ultimate stress in compression measured in each system. This was done in order to avoid damage to the transducer in case of brittle or explosive failure. Secant modulus of elasticity was calculated according to the procedure in EC2. Accordingly, the modulus of elasticity refers to the slope of the stress-strain obtained between the origin and 40% of the ultimate stress in compression, determined in accordance with ASTM standard – C39. Cylinders measuring 60 mm in diameter and 120 mm height containing high performance cement pastes were prepared for measurement at 6 different curing times. Ultimate strength refers to an applied load rate of 0.71 MPa s^{-1}. The results shown refer to the strength values taken at 28 days hardening time in sealed curing. Tensile strength was derived from 4-point bending. Tests were performed in accordance with EN 12390-5:2009, using 240 mm long thin plates with a cross section of 60 × 5 mm, a span of 100 mm, and a force applied at 2 positions.

The experimental characterization was undertaken for several concentrations of SAP, which provides different quantities of bubbles. These bubbles provide an increase in the overall porosity of the cement mixture. The analysed systems and their results are collected in Table 1. This table includes three columns about the level of porosity expressed in different manners: a first column with the weight percentage of SAP in the mixture, a second column with the equivalent volume percentage of this SAP porosity and a third column with the volume percentage of total porosity, which is composed by a the cement porosity (about 28%) and an additional porosity due to SAP. Therefore the total porosity for a case is obtained as: $\textit{Cement porosity} \cdot (1 - \textit{Void SAP}) + \textit{Void SAP}$.

3. Modelling methodology

The prediction of effective properties for a composite material, using continuum micromechanics, involves several steps: knowledge of the microstructure and reconstruction of the corresponding RVE, recognition of the different constituents and use of suitable material models and properties for each phase, and finally calculation of the effective material behaviour under the desired loading conditions. In this study a numerical approach based on FEM has been used due to its advantage (as note above) over the analytical or empirical approaches [1].

In order to define the RVE, the microstructure of the porous cement material is identified via a computerized tomography, being the PSD of the porosity obtained using absorbency measurements (described in the previous section). On the basis of these observations, the different phases of the material are identified, where a phase is the part of the domain that can be identified at a given scale with constant material properties [20]. The microstructure of the porous cement-based material analysed at micro-scale, is considered composed of two phases: cement paste and spherical voids generated by SAP, as shown in Fig. 1. The cement paste at micro-scale is assumed herein to be a homogeneous material, although at lower scales it also has a heterogeneous structure resulting from the cement recipe and hydration process. Based on this information on the micro-scale, the reconstruction of the corresponding RVE is undertaken as described in following subsection.

From a theoretical point of view, random heterogeneous materials, such as the one of study, were deeply investigated by Torquato [21]. He went in the Part I of the book into details about the characterization of the microstructure including the analysis distribution and packing of spherical particles, considering non-overlapping/overlapping or clustering.

3.1. Geometry and mesh

The RVE which satisfies the determined morphology characteristics conditions is generated using Digimat [22], which is a commercial software focused on linear and non-linear multi-scale material modelling. Among others, it has a module, called Digimat-FE, for generating the geometry of the microstructure based on: content of heterogeneities, size of the particles and distribution. The inclusions or voids are allocated by a random dispersion but accomplishing the requirements about distribution, content, periodic geometry, etc.

Along this paper the generation of the RVE for the porous cement material is performed considering a matrix of cement paste where the inclusions are voids associated with the bubbles generated by SAP. These bubbles have a spherical shape with a PSD, as noted in the Porous cement-based materials by superabsorbent polymers section. The definition of the PSD in terms of % of particles versus size is shown in Fig. 2.

In addition to the PSD, the RVE generation process requires the definition of the content of inclusions in terms of volume fraction and topological information on inclusion dispersion. In this study, good bubble dispersion has been assumed because no clusters are observed in the tomography (Fig. 1). This factor is included in RVE generation by considering a uniform dispersion around the RVE. A further typical characteristic of heterogeneous materials with voids is the overlapping of the inclusions, such as described Torquato [21], which is not considered for this microstructure because their formation mechanism, from swollen solid SAP particles, does not allow it. The RVE is created under these considerations; a reconstruction for a 25% volume fraction of voids generated by SAP is shown in Fig. 3.

Another equally important parameter is the characteristic length of the RVE (or RVE size), which has repeatedly been investigated as Gitman et al. have summarised [23]. Theoretically, the RVE must be large enough compared to the dimension of the heterogeneities yet small enough compared to the system analysed. Pelissou [24] affirmed that there is not a priori a criteria to determine the minimum RVE size because it depends on the material structure, on the volume fraction of heterogeneities and on other characteristics of the microstructure. Normally, a lager RVE tends to provide more accurate prediction, but there is a minimum RVE where the solution converges within a tolerance [3]. Therefore, this parameter of the material object of study is analysed herein; the details of it are given in Application of the methodology section.

Working with this geometry, the RVE mesh is generated by using Abaqus-CAE [25], a commercial pre/post processor for FEM analysis. The RVE mesh is defined with linear tetrahedral elements, which are generated taken into account the following meshing parameters

Table 1
Experimental characterisation.

SAP system [%]	Voids SAP [%]	Total porosity [%]	Elastic mod. [GPa]	Comp. strength [MPa]	Flexural strength [MPa]
0.00	0.00	27.7	37.0	102	8.00
0.25	13.0	36.5	–	79.1	6.60
0.50	20.0	41.6	22.8	52.1	5.80
1.00	32.0	50.4	16.2	25.2	4.20
2.00	50.0	63.5	9.90	14.1	2.60

Please cite this article as: I. Viejo et al., Numerical modelling of porous cement-based materials by superabsorbent polymers, Cement and Concrete Research (2016), http://dx.doi.org/10.1016/j.cemconres.2016.07.018

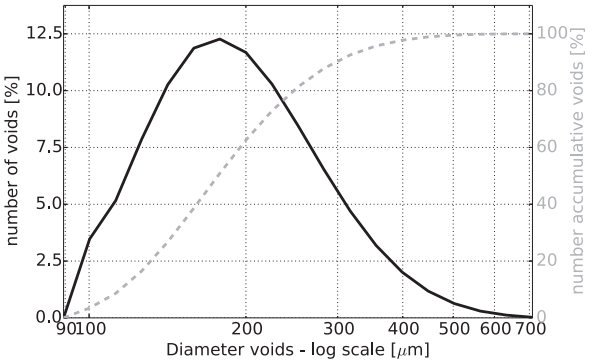

Fig. 2. Particle size distribution of the swollen SAP in terms of percentage of particles and the accumulative value of this variable. The average swollen size is about 175μm.

which control the quality of the mesh: element size, deviation factor, minimum size factor and size growth. In order to obtain a compromise between quality and computational cost, several influence analysis have been undertaken to fix these parameters.

3.2. Boundary conditions

The boundary conditions (BC) are also an important factor affecting the solution [3,26,27], being also its influence related to RVE size. The minimum RVE size providing a stable prediction is different depending on boundary conditions used.

In this paper, periodic boundary conditions are employed, formulated as described by Doghri [28]. This type of boundary condition imposes relative displacements between opposite sides, such that neighbouring cells fill all space leaving no gaps under any strain state. In this case, the RVE geometry has to be also periodic. This type of BC ensures that the variation in the displacement is periodic with respect to all sides of the volume element [29]. Several papers have shown that this type of boundary conditions requires a smaller RVE size than with other boundary conditions [3,23,24,28].

The criterion used for the definition of the RVE size has been established based on the analysis of a RVE with the same characteristics (total porosity about 35%), but with different side length, from 1.75 mm to 3.5 mm. The prediction has been performed for five different RVEs with the same length, obtaining the mean value and the standard deviation in terms of elastic modulus and strengths. The RVE size has been established based in the difference in the mean values. For this level of porosity, a RVE of 2.75 mm side length gives an error lower than 5% in strength and 1% in the elastic modulus with regard to the case of 3.5 mm. Once the RVE size is fixed for this level of porosity, the RVE size for other levels of porosity is established in order to include the same number of voids. The number of inclusions for the 2.75 mm RVE is about 350, which is significantly higher than the recommended by other authors for obtaining the same 5% error, which was 30 inclusions [30–32].

3.3. Material model

Once the RVE geometry is generated, the definition of the proper material models for each constituent is undertaken to feed the prediction approach. For the particular material being studied, only the material model of the cement paste has been defined, because the inclusions are voids without mechanical stiffness and strength. The material model chosen to describe the behaviour of the cement paste is a damage plasticity model- typically used to represent concrete. This model is available in the library of the FEM code used in this study: Abaqus [25]. This material model, mainly intended for quasi-brittle materials, is defined in terms of the stress-strain curves under pure tensile and compression uniaxial tests.

The pure uniaxial stress-strain response is shown in the scheme of Table 1. Under uniaxial tension, the material response consists in a linear elastic relationship (E) until the value of failure stress (σ_{t1}) is reached. Beyond this failure, a softening stress-strain relation is introduced characterized by σ_{t2} and ϵ_{t2}. Under uniaxial compression the material has the same elastic response after the yield stress is reached, followed by a plastic regime, until ultimate stress (σ_{c1}), and a subsequent softening characterized by σ_{c2} and ϵ_{c2}. In this paper, the plastic regime is not considered by defining the yield stress approximately equal to the ultimate stress because the cement paste has not a plastic regime. Beyond the ultimate stresses σ_{t1} and σ_{c1}, the stiffness is also reduced by the damage parameters. This description characterises the behaviour at each integration point of the FE model.

In order to obtain the parameters of this damage plasticity model, reverse engineering is performed using two experimental

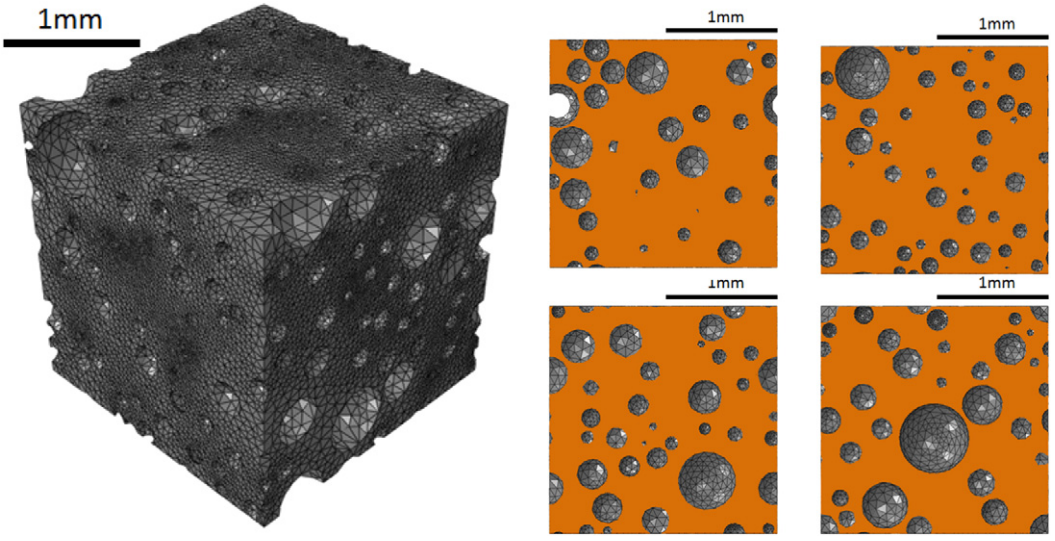

Fig. 3. RVE with previous characteristics considering void content of 25% (RVE size=2.05mm) and the FE mesh of this RVE. Left: perspective view of this RVE. Right: several slices of the same RVE in left.

Please cite this article as: I. Viejo et al., Numerical modelling of porous cement-based materials by superabsorbent polymers, Cement and Concrete Research (2016), http://dx.doi.org/10.1016/j.cemconres.2016.07.018

Table 2
Cement paste material model.

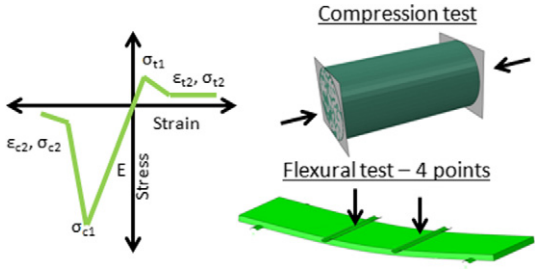

Parameter	Value
Elastic modulus (E)	37 GPa
Tensile strength (σ_{t1})	3.15 MPa
Damage model tensile: σ_{t2}	0.75 MPa
Damage model tensile: ϵ_{t2}	8E–03
Compressivestrength(σ_{c1})	102.0 MPa
Damage model compression: σ_{c2}	10.00 MPa
Damage model compression: ϵ_{c2}	6E–03

tests (uniaxial compression and flexural tests) for the same cement mixture but without SAP. This reverse engineering is performed by means of FEM models with the same specimen dimensions, loading and using boundary conditions equivalent to the experimental test setup. Lastly, the parameters of this model are fitted sequentially: first, using uniaxial compression test data to obtain elastic modulus (initial tangent modulus and secant modulus showed the same value) and compressive strength, and second, flexural test data to determine tensile strength. The final parameters of the material model equivalent to the cement mixture without SAP are included in Table 2. In addition, the relation between tensile and flexural strength, that is used to convert the flexural strength data in Table 1 to tensile strength, is obtained. This ratio is around 2.5, that is consistent with the literature for cement-based materials 33–34.

3.4. Prediction

The prediction of the overall mechanical behaviour is performed by computing the overall stress-strain response from the reaction forces and displacement in the boundary conditions. This type of estimation provides similar results that the volumetric average in terms of stresses or strains for linear behaviour, which is common in FE micromechanics, cf. [31]. In this paper, in which the damage of the material has been included, the overall stress-strain response is calculated from the reaction force divided by the RVE area and the displacement divided by the RVE length, as Bernard used also for a cement-based material [1]. From the stress-strain curve, the elastic modulus is obtained as the initial tangent modulus, which gives nearly same value that secant modulus at 40% of the ultimate compression strength. The difference between these two modulus was less than 0.5%. Also the tensile and compressive strengths are extracted from this curve taking the absolute maximum and minimum stresses. Due to the brittle nature of cement-based materials, these three parameters allow its essential mechanical behaviour to be described. Additionally, FE micromechanics provides the capability to analyse the local stresses or other variables, such as damage, that provide information about the deformation mechanism of a porous cement-based material.

4. Application of the methodology

The described modelling methodology is applied to the prediction of the porous cement-based material of this study. The results obtained are compared with the experimental characterization test data given in Table 1.

In order to compare the prediction for effective behaviour with that of the experimental results, different RVE with distinct quantities of voids are analysed. Given the feasibility of the modelling procedure, the numerical prediction analyses a greater number of cases than experiments available; several repetitions (between 3 and 5) using similar void content are calculated to check repeatability in the predictions. This type of repetition using identical microstructure characteristics is frequent in FE micromechanics analysis to check dispersion in the predictions due to the random nature of the microstructure geometry generation process [3].

The methodology is applied, generating 29 RVEs with voids content between 2.5% and 30%. The results of the prediction of effective properties are collected in Fig. 4. It can be appreciated that while the prediction for the elastic modulus and tensile strength present a reasonable accuracy in terms of trends, the results in compressive strength differ significantly. In the following section, these results are analysed in order to understand the behaviour of the porous cement and explain the differences observed, specially at low concentration for compressive strength.

The RVE with highest level of porosity was about 30% of void content, lower than the theoretically maximum packing of spheres [21]. This limitation proceeds from the approach used for the geometry generation, the parameters in that generation (such as the minimum distance between inclusions that avoid the generation of clusterings) and the micro-structure information used as input such as the PSD. The algorithm is not able to include additional pores fulfilling with all the constraints. Relaxing the constraints, it would be possible to reach higher percentage of void content but it is considered unrealistic and discarded.

Besides previous results, FE micromechanics provides the possibility of analysing the local behaviour of the microstructure, including local stresses or local failure close to voids. The analysis is mainly undertaken in terms of stresses (maximum and minimum principal)

Please cite this article as: I. Viejo et al., Numerical modelling of porous cement-based materials by superabsorbent polymers, Cement and Concrete Research (2016), http://dx.doi.org/10.1016/j.cemconres.2016.07.018

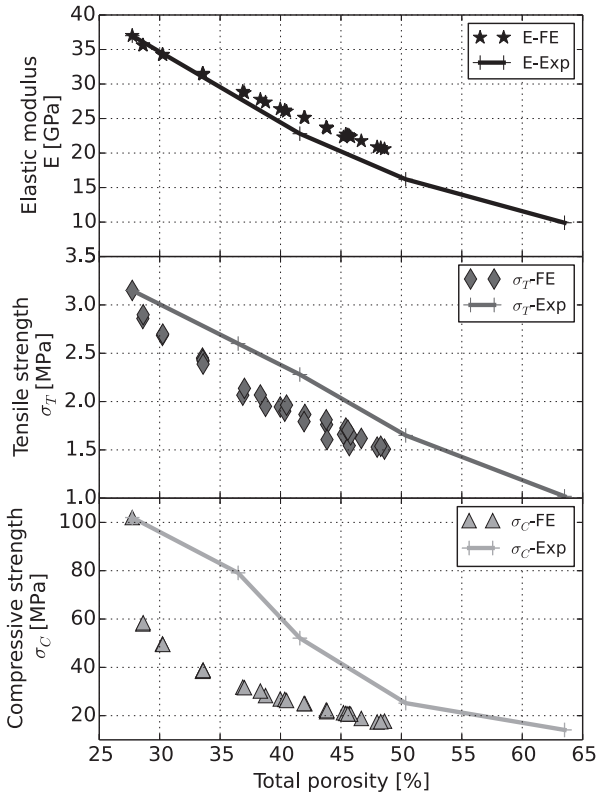

Fig. 4. Prediction with the SAP system for elastic modulus, tensile strength and compressive strength versus total porosity (cement paste porosity and additional porosity generated by SAP).

and the damage. The latter represents the 'degradation' of the cement when the tensile or compressive strength is locally reached, and it splits in two damage variables, one for tensile (DAMAGET) and one for compression (DAMAGEC). A not null value means that the tensile or compressive strength has been exceeded, and therefore, the damage has started.

Under tensile loads, all RVEs analyzed fail by the cross section, transversal to the load, that presents the highest voids area, that is, the smallest neat cement area. In Fig. 5 (a), the damage variable shows on red colour the zone where the tensile strength has been reached, creating a percolated damaged section, that could well represent a transversal crack. Within this section, the zone which reaches the maximum tensile stress is almost always located between two voids which are very close together.

Under compression loads (Fig. 5 (b)) more diffuse damage pattern appears, presenting both, damage in tension and compression. However, as the strength of the cement is much lower under tension, the local failure in the microstructure starts due to the tensile stresses. This effect will be clearly observed in the sensitivity analysis (see Sensitivity analysis section) for the cement matrix properties, showing that changes in the tensile strength of the cement have a significant influence on the compressive strength of the cement with pores.

5. Discussion

As can be seen in Fig. 4, the predicted effective properties have registered a significant difference in terms of compressive strength. In order to understand the cause behind these differences and the behaviour of the porous cement-based material, previous results are analysed and discussed in different ways.

First, the predicted and experimental results versus total porosity are fitted to different regressions curves. These curves are compared with the analytical expression that has been used in literature for cement materials and porous cement materials. The regression curves used in the adjustment are linear, exponential and power-law. In the case of power-law regression, it is undertaken considering the abscissas ($1 - \textit{total porosity}$). Table 3 shows the different curves and the coefficient of determination (or R-squared) in order to quantify how well the data fit the regression. The fittings with the power-law are shown in Fig. 6, that, as it will be explained, is the regression that best fit.

Based on the R-squared, the elastic modulus could be fitted by the 3 regressions analysed with similar values of R-squared, with the exception of the linear regression for the experimental data. By comparing those that fit with the approaches in the literature, a correspondence has been found with a power-law for closed-cell cellular solids in Gibson [16] and with the three regressions for concrete in Yaman [15]. Furthermore, Roberts [35] gives an indication of the range for parameter b for the power-law regression, which in general is in the range of $1 < b < 4$ although that for closed-cell foams some experimental studies indicate a range of $1 < b < 2$. The values of parameter b in the present study are 1.92 for experimental data and 1.68 for FE prediction, both within the range indicated by Roberts. Therefore, the Elastic modulus prediction with the proposed methodology is coherent with the literature and, with slight differences, adjusts to the experimental data.

For the tensile strength, the best fitting with the experimental data is achieved with power-law or even linear regression, both showing a similar R-squared value. However, the numerical prediction is best approached using either exponential or perhaps power-law regression. Although linear regression shows a high R-squared value, this regression does not correctly adjust the lowest and highest porosity values. The study of tensile strength is not very habitual for cement materials, however Balshin [36] employed a power-law for establishing a relation between the porosity and the tensile strength but not reference values are given.

Finally, in terms of the compressive strength, the best adjustment for experimental data and numerical prediction is achieved using exponential regression, although power-law regression is also possible as, it only has a slightly lower R-squared value. However, no regression has been found to adjust the case of zero SAP porosity (total porosity 28%). In the literature, the most commonly used expression to adjust compressive strength for cement-based materials is a power-law, likewise the models based on Balshin's model and Powers' gel-space ratio equation. Using this type of models, Nambiar [17] summarizes the value of the constants for some mixtures. The exponent (b) has a range of 1.8 to 4.3 while the constant (a) ranges of 25 to 290. Thus, the values for both parameters in the present study lie within the range for cement-based materials.

As explained above, the difference in terms of compressive strength between the numerical prediction and the experimental characterization is significant. This difference could result from different factors, among them some initial assumptions made in the modelling.

One of the main assumptions made in previous modelling approach is that the microstructure comprises two phases: cement paste and voids generated by SAP on the micro-scale. Therefore, the cement paste, that includes different additives and the intrinsic porosity mainly on the nano-scale (in this paper 28% as was measurement in Porous cement-based materials by superabsorbent polymers section for case without SAP), is being considered as homogeneous material at micro-scale. Given that the voids generated by SAP and the porosity of the cement paste are at different scales, the initial assumption of homogenized cement paste including its porosity could have been reasonable. Consequently, the low prediction in terms of compressive strength, that was displayed in Fig. 4, may arise

Please cite this article as: I. Viejo et al., Numerical modelling of porous cement-based materials by superabsorbent polymers, Cement and Concrete Research (2016), http://dx.doi.org/10.1016/j.cemconres.2016.07.018

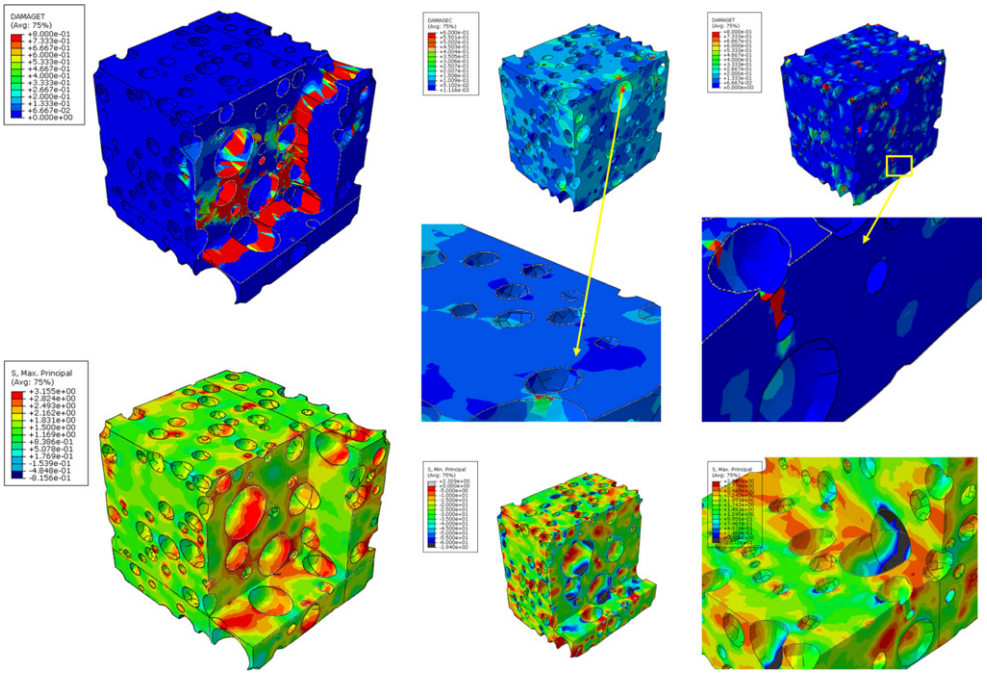

(a) Under tensile uniaxial load (Top: DAMAGET. Bottom: Maximum principal stress.)

(b) Under compression uniaxial load (Top: DAMAGEC / DAMAGET. Bottom: Minimum/Maximum principal stress.)

Fig. 5. Contour distribution for an RVE with 43.8% of total porosity under uniaxial loads for damage variables and maximum/minimum principal stresses.

from this assumption. It is especially noticeable at cases with lowest total porosity that include SAP voids, is said case with 28.6% total porosity (or 2.5% of voids SAP). These cases only increase the total porosity 0.87% (from 27.73% to 28.60%) but the predicted compressive strength is reduced about 43% (from 102 MPa to about 58 MPa). On the other hand, the experimental results exhibited that increasing the total porosity 8.76% (from 27.73% to 36.49%) reduces the compressive strength 22.5% (from 102 MPa to 79.10 MPa). Therefore the variation between no SAP voids and the lowest percentage of voids measured for experimental results is smoother than the predicted with the FE model. This fact was highlighted by Esteves [37] when reviewing the classic model approaches. On the basis of previous statements, the intrinsic porosity associated with the cement paste has a notable impact on the compressive strength and, a modelling including it, should be more accurate.

A FE model (or RVE) including explicitly voids of the cement paste and voids of SAP is not affordable due to the differences in the size of the two types of voids, that are at different scales. The limitations would be found in the geometry generation, in order to allocate a higher level of total porosity, in the mesh generation, due to the very small element size required for the voids of the cement paste, and in the calculation procedure, due to the huge computational resources required by a very fine mesh.

In order to address the modelling of both types of voids, an attempt has been made to include indirectly the porosity associated with cement paste to the current modelling approach (Section 3). This alternative modelling approach consists in re-fitting the cement paste properties of the compression behaviour that was fitted in Material model section. This is made by increasing compressive strength σ_{C1} until the compressive strength predicted for a RVE with a total porosity of 36.49% (13% SAP porosity) reaches to 79.10 MPa (the value measured for this SAP porosity case: *SAP system 0.25%* in Table 1). The ϵ_{C2} parameter is recalculated to maintain the slope at the softening regime. Once the new FE material model is obtained, several RVEs at different levels of porosity are recalculated. The comparative of this new prediction against the experimental and previous prediction is shown in Fig. 7. The new prediction captures well the trend when additional porosity is added. Therefore, the relative increase of porosity at same size scale is predicted correctly by the model. To say this, the cement paste intrinsic porosity is not required to be included because the relative increase is predicted properly (FE-adjusted model). Nevertheless, the cement paste

Table 3
How the predicted and experimental results fit into regression curves.

		Linear: $Y = a \cdot x + b$			*Exponential:* $Y = a \cdot exp(b \cdot x)$			*Power-law:* $Y = a \cdot x^b$		
		a	b	R^2	a	b	R^2	a	b	R^2
E	EXP	−75.9	56.3	0.967	104	−3.69	0.999	66.0	1.93	0.991
	FE	−76.5	57.3	0.997	78.7	−2.74	1.000	62.6	1.68	1.000
Tensile strength - σ_T	EXP	−6.03	4.80	0.995	8.15	−3.20	0.987	5.50	1.67	0.998
	FE	−6.93	4.78	0.963	7.19	−3.24	0.980	5.49	1.99	0.970
compressive strength - σ_C	EXP	−264	171	0.923	600	−5.98	0.978	281	3.09	0.965
	FE	−232	122	0.750	348	−6.28	0.943	204	3.83	0.920

Please cite this article as: I. Viejo et al., Numerical modelling of porous cement-based materials by superabsorbent polymers, Cement and Concrete Research (2016), http://dx.doi.org/10.1016/j.cemconres.2016.07.018

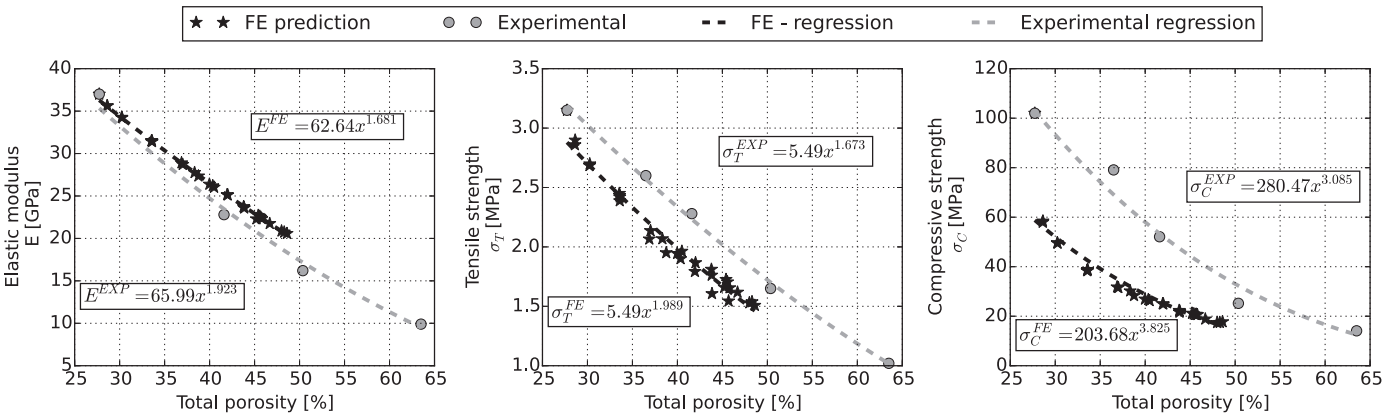

Fig. 6. Predicted and experimental results fitted by power-law regression.

cannot be assumed as an equivalent homogeneous material explicitly that includes its intrinsic porosity, because the prediction is overestimated (FE model).

Therefore, the defined model in Section 3 can be useful to analyse a porous-cement based material, but the cement paste properties of the FE model has to be fitted for a case that includes the intrinsic porosity of the cement paste and additional porosity with SAP.

6. Sensitivity analysis

For cement-based materials, material properties are wholly influenced by the additives, process, water content, and even the dispersion between samples. Therefore, the desired properties for a specific cement-based material with SAP can be achieved by combining, i.e. cement paste properties without SAP and the characteristics of SAP: PSD, content, distribution, etc. The influence of the SAP content has been studied previously, consequently in this section, the influence of the material properties and other SAP parameters are analysed. Although this type of sensitivity analysis can be performed by means of experimental characterization, numerical modelling can help to accelerate the work process.

The sensitivity analysis for the cement paste properties is undertaken by considering different tensile and compressive stress-strain curves for the matrix. In this study, these changes in the stress-strain curves are defined by considering a 25% increase or decrease in the tensile (σ_{t1}) and compressive (σ_{c1}) strength curves on an individual basis, the rest of material parameters are modified to have the same softening slope. This study has been carried out for five RVEs with different total porosity content (33.6%, 37.0%, 38.7%, 41.9% and 45.9%) in order to show an overall trend.

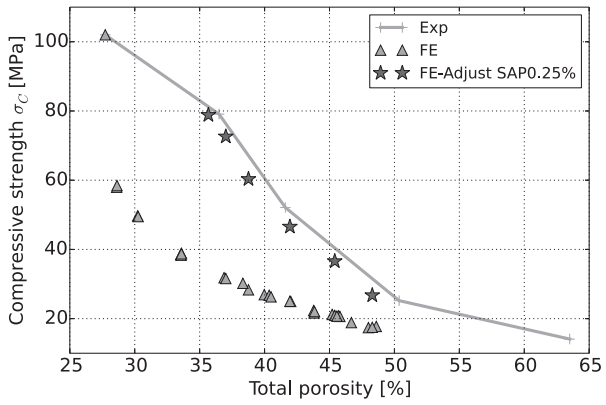

Fig. 7. Prediction with the SAP system for compressive strength versus total porosity (cement paste porosity and additional porosity generated by SAP) using the refitting material model.

The prediction in terms of tensile strength is compared with the value obtained with the original material model. It has been found that the percentage of reduction/increase in the value of σ_{t1} is directly proportional to the reduction/increase in the tensile strength predicted by the RVE. The modification of compressive parameters (σ_{c1}) has not an effect on the tensile strength, see Fig. 8. This substantiates the readjustment of the material model from the previous section, not affecting to the tensile predictions.

On the other hand, the compressive strength predicted for the foamed cement material is influenced by the compressive (σ_{c1}) and tensile (σ_{t1}) strength properties of the cement paste. This is the result of the local effects showing the presence of tensile and compressive damage when the RVE is under uniaxial compression load (see Application of the methodology section). A summary of this influence is collected in Fig. 8. In addition, this influence is also dependent on the total porosity.

Previous analysis of this paper considered porous cement material with a pore size distribution based on measured data. However, this porous material could be produced using SAP of different diameters, even constant, it depends in the SAP introduced at the mixture process. Subsequently, the influence of the pore size at micro scale in the effective properties is evaluated considering porous cement-based materials by SAP of different pore size. Three constant pore size diameters were considered: 100 μm, 200 μm and 300 μm. For each one of these diameters, five RVEs have been built for a total porosity of about 40%. The results are compared with previous results undertaken with PSD with similar SAP content. Table 4 summarizes the results in terms of mean and standard deviation of the five RVEs for each combination. It is concluded that the pore size has no significant influence on the elastic modulus and tensile strength. However, compressive strength is slightly reduced as a function of the increase in SAP size. Also this has been observed experimentally using SAP with different diameters (for a total porosity of 38%). The strength variation compared to the system with no SAP was considered a parameter with significance: 50–75 μm (−6%), 75–125 μm (−12%), 125–150 μm (−17%), 150–180 μm (−18%) [37].

7. Conclusion

A 3D modelling approach based on computational micromechanics is presented to predict the mechanical behaviour of porous cement-based materials by SAP. The proposed approach provides a quantitative means to estimate and predict the mechanical properties of porous cement materials taking into account the micro-structure.

Please cite this article as: I. Viejo et al., Numerical modelling of porous cement-based materials by superabsorbent polymers, Cement and Concrete Research (2016), http://dx.doi.org/10.1016/j.cemconres.2016.07.018

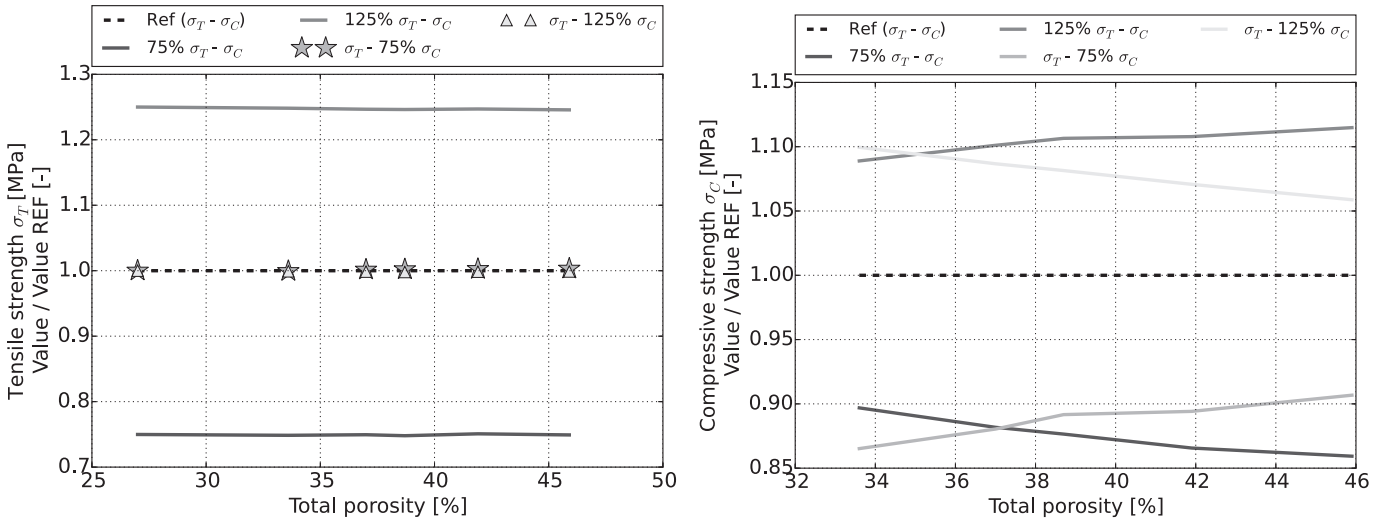

Fig. 8. Influence of the cement paste material properties in tensile and compressive strength at different porosity level. Ordinate axis shows the ratio between the strength with the new material properties and the strength with the reference material. Abscissae axis shows the total porosity.

Table 4
Influence of the pore size. Values are given as the mean and standard deviation of several cases with similar definition of SAP voids and pore size.

Pore size [μm]	Total porosity [%]	E [GPa]	Tensile strength [MPa]	Comp. strength [MPa]
PSD (mean = 175)	40.28 ± 0.27	26.20 ± 0.18	1.94 ± 0.03	26.64 ± 0.33
100	40.24 ± 0.51	26.40 ± 0.60	1.97 ± 0.03	28.20 ± 1.82
200	40.52 ± 0.31	26.20 ± 0.38	1.93 ± 0.04	27.20 ± 0.96
300	40.53 ± 0.30	26.18 ± 0.34	1.96 ± 0.04	26.69 ± 1.54

The results indicate that the elastic and tensile strength predictions are satisfactory using, in the material model adjustment, the characterization of the cement paste without SAP. However, for obtaining a good prediction of the compressive strength, the material model has to be fitted using the characterization of any case with SAP voids in order to indirectly include the intrinsic porosity associated with the cement paste. The relation between the mechanical property and the porosity is well fitted by a power-law equation, both for experimental and numerical predictions, being fitted the parameters in the same range that has previously been found out by other researchers for other type of cement-based materials.

The relation between the cement paste properties and the porous cement-based material has been established through the numerical approach. The compression strength of the porous cement material is strongly influenced by both tensile and compression strength of cement paste. This fact is directly related with the observation in the stress and damages distributions under compression loads, in which tensile and compression damage appear around the pores. On the other hand, the behaviour of the porous material under pure tensile loads is directly influenced by cement paste tensile strength and the minimum cross section transversal to the load. Additionally to this relations, the influence of the pore size effect was evaluated with the approach, obtaining that the pore size has not effect in the elastic modulus and tensile strength, and that, an increase in the pore size provokes a slight reduction of the compression strength.

The good correlation between experimental and numerical results shows the utility of including the proposed modelling approach in the development of this type of material, in order to reduce the number of experimental tests, and to optimize the microstructure characteristics. Nevertheless, this modelling approach requires improvements in order to be able to consider total porosity above 50% and even to model cement paste porosity directly.

Acknowledgements

This research was partly supported by the European Commission funding of the FIBCEM project (grant no.: 262954).

References

[1] F. Bernard, S. Kamali-Bernard, W. Prince, 3D multi-scale modelling of mechanical behaviour of sound and leached mortar, Cem. Concr. Res. 38 (4) (2008) 449–458. http://dx.doi.org/10.1016/j.cemconres.2007.11.015.
[2] A.P. Roberts, E.J. Garboczi, Elastic properties of model porous ceramics, J. Am. Ceram. Soc. 83 (12) (2000) 3041–3048. http://dx.doi.org/10.1111/j.1151-2916.2000.tb01680.x.
[3] T. Kanit, S. Forest, I. Galliet, V. Mounoury, D. Jeulin, Determination of the size of the representative volume element for random composites: statistical and numerical approach, Int. J. Solids Struct. 40 (13-14) (2003) 3647–3679. http://dx.doi.org/10.1016/S0020-7683(03)00143-4.
[4] O. Bernard, F.-J. Ulm, E. Lemarchand, A multiscale micromechanics-hydration model for the early-age elastic properties of cement-based materials, Cem. Concr. Res. 33 (9) (2003) 1293–1309. http://dx.doi.org/10.1016/S0008-8846(03)00039-5.
[5] N. Moussaif, I. Viejo, J.M. Bielsa, C. Crespo, S. Irusta, C. Yagüe, J.G. Meier, Preparation, characterization and FE-simulation of the reinforcement of polycaprolactone with PEGylated silica nanoparticles, IOP Conf. Ser. Mater. Sci. Eng. 40 (2012) 012026. http://dx.doi.org/10.1088/1757-899X/40/1/012026.
[6] B. Bary, M.B. Haha, E. Adam, P. Montarnal, Numerical and analytical effective elastic properties of degraded cement pastes, Cem. Concr. Res. 39 (10) (2009) 902–912. http://dx.doi.org/10.1016/j.cemconres.2009.06.012.
[7] V. Šmilauer, Z. Bittnar, Microstructure-based micromechanical prediction of elastic properties in hydrating cement paste, Cem. Concr. Res. 36 (9) (2006) 1708–1718. http://dx.doi.org/10.1016/j.cemconres.2006.05.014.

[8] L. Sorelli, G. Constantinides, F.-J.J. Ulm, F. Toutlemonde, The nano-mechanical signature of ultra high performance concrete by statistical nanoindentation techniques, Cem. Concr. Res. 38 (12) (2008) 1447–1456. http://dx.doi.org/10.1016/j.cemconres.2008.09.002.

[9] M.G. Hernández, J.J. Anaya, L.G. Ullate, A. Ibañez, Formulation of a new micromechanic model of three phases for ultrasonic characterization of cement-based materials, Cem. Concr. Res. 36 (4) (2006) 609–616. http://dx.doi.org/10.1016/j.cemconres.2004.07.017.

[10] M. Acebes Pascual, Estudio y extensión de un modelo micromecánico trifásico para la caracterización ultrasónica de materiales compuestos, Universidad Politécnica de Madrid. 2007. (Ph.D. thesis)

[11] S. Kamali, M. Moranville, E. Garboczi, S. Prené, B. Gérard, Hydrate dissolution influence on the Young's modulus of cement pastes, Proceedings of the 5Th International Conference on Fracture Mechanics of Concrete and Concrete Structures, April 2004, pp. 12–16.

[12] C.-J. Haecker, E.J. Garboczi, J.W. Bullard, R.B. Bohn, Z. Sun, S.P. Shah, T. Voigt, Modeling the linear elastic properties of Portland cement paste, Cem. Concr. Res. 35 (10) (2005) 1948–1960. http://dx.doi.org/10.1016/j.cemconres.2005.05.001.

[13] C. Toulemonde, R. Masson, J. El Gharib, Modeling the effective elastic behavior of composites: a mixed finite element and homogenisation approach, C.R. Mec. 336 (3) (2008) 275–282. http://dx.doi.org/10.1016/j.crme.2007.11.024.

[14] S.-M.M. Kim, R.K. Abu Al-Rub, Meso-scale computational modeling of the plastic-damage response of cementitious composites, Cem. Concr. Res. 41 (3) (2011) 339–358. http://dx.doi.org/10.1016/j.cemconres.2010.12.002.

[15] I.O. Yaman, H.M. Aktan, N. Hearn, Active and non-active porosity in concrete Part II: evaluation of existing models, Mater. Struct. 35 (2) (2002) 110–116. http://dx.doi.org/10.1007/BF02482110.

[16] L. Gibson, M. Ashby, Cellular solids: structure & properties, Adv. Polym. Technol. 9 (2) (1989) 165–166. http://dx.doi.org/10.1002/adv.1989.060090207.

[17] E.K.K. Nambiar, K. Ramamurthy, Models for strength prediction of foam concrete, Mater. Struct. 41 (2) (2008) 247–254. http://dx.doi.org/10.1617/s11527-007-9234-0.

[18] L.P. Esteves, O.M. Jensen, Design of porous cement-based materials - defining a research context in FIBCEM report 3.2, Tech. Rep., Nanotechnology Enhanced Extruded Fibre Reinforced Foam Cement based Environmentally Friendly Sandwich Material for Building Applications, EU FP7 THEME NMP-2010-1.2-2, Grant Agreement no. 262954., 2012,

[19] L.P. Esteves, Recommended method for measurement of absorbency of super-absorbent polymers in cement-based materials, Mater. Struct. 48 (8) (2015) 2397–2401. http://dx.doi.org/10.1617/s11527-014-0324-5.

[20] A. Zaoui, Continuum micromechanics: survey, J. Eng. Mech. 128 (8) (2002) 808–816. http://dx.doi.org/10.1061/(ASCE)0733-9399(2002)128:8(808).

[21] S. Torquato, Random Heterogeneous Materials, 1st edition ed., Interdisciplinary Applied Mathematics vol. 16. Springer New York, New York, NY, 2002. http://dx.doi.org/10.1007/978-1-4757-6355-3.

[22] E.-X. engineering, Digimat Version 5.1.1, Linear and Nonlinear Multi-scale Material Modeling Software, 2014, http://www.e-xstream.com.

[23] I. Gitman, H. Askes, L. Sluys, Representative volume: existence and size determination, Eng. Fract. Mech. 74 (16) (2007) 2518–2534. http://dx.doi.org/10.1016/j.engfracmech.2006.12.021.

[24] C. Pelissou, J. Baccou, Y. Monerie, F. Perales, Determination of the size of the representative volume element for random quasi-brittle composites, Int. J. Solids Struct. 46 (14-15) (2009) 2842–2855. http://dx.doi.org/10.1016/j.ijsolstr.2009.03.015.

[25] Dassault Systèmes, Abaqus v6.12. - General Purpose FE Software, 2013, http://50.16.225.63/.

[26] Z.F. Khisaeva, M. Ostoja-Starzewski, On the size of RVE in finite elasticity of random composites, J. Elast. 85 (2) (2006) 153–173. http://dx.doi.org/10.1007/s10659-006-9076-y.

[27] X. Yue, E. Weinan, The local microscale problem in the multiscale modeling of strongly heterogeneous media: effects of boundary conditions and cell size, J. Comput. Phys. 222 (2) (2007) 556–572. http://dx.doi.org/10.1016/j.jcp.2006.07.034.

[28] I. Doghri, M. El Ghezal, L. Adam, Finite strain mean-field homogenization of composite materials with hyperelastic-plastic constituents, Int. J. Plast. 81 (2016) 40–62. http://dx.doi.org/10.1016/j.ijplas.2016.01.009.

[29] J. Segurado, J. Llorca, A numerical approximation to the elastic properties of sphere-reinforced composites, J. Mech. Phys. Solids 50 (10) (2002) 2107–2121. http://dx.doi.org/10.1016/S0022-5096(02)00021-2.

[30] J. Segurado, J. Llorca, C. González, On the accuracy of mean-field approaches to simulate the plastic deformation of composites, Scr. Mater. 46 (7) (2002) 525–529. http://dx.doi.org/10.1016/S1359-6462(02)00027-1.

[31] O. Pierard, C. González, J. Segurado, J. LLorca, I. Doghri, Micromechanics of elasto-plastic materials reinforced with ellipsoidal inclusions, Int. J. Solids Struct. 44 (2007) 6945–6962. http://dx.doi.org/10.1016/j.ijsolstr.2007.03.019.

[32] L. Brassart, I. Doghri, L. Delannay, Homogenization of elasto-plastic composites coupled with a nonlinear finite element analysis of the equivalent inclusion problem, Int. J. Solids Struct. 47 (5) (2010) 716–729. http://dx.doi.org/10.1016/j.ijsolstr.2009.11.013.

[33] M. Maalej, V.C. Li, Flexural/tensile strength ratio in engineered cementitious composites, J. Mater. Civ. Eng. 6 (4) (1994) 513–528. http://dx.doi.org/10.1061/(ASCE)0899-1561(1994)6:4(513).

[34] X. Chen, S. Wu, J. Zhou, Influence of porosity on compressive and tensile strength of cement mortar, Construct. Build Mater. 40 (2013) 869–874. http://dx.doi.org/10.1016/j.conbuildmat.2012.11.072.

[35] A. Roberts, E. Garboczi, Elastic moduli of model random three-dimensional closed-cell cellular solids, Acta Mater. 49 (2) (2001) 189–197. http://dx.doi.org/10.1016/S1359-6454(00)00314-1.

[36] M.Y. Balshin, Relation of mechanical properties of powder metals and their porosity and the ultimate properties of porous metal-ceramic materials, Dokl. Akad. Nauk SSSR 67 (5) (1949) 831–834.

[37] L.P. Esteves, An ongoing investigation on modeling the strength properties of water-entrained cement-based materials, Concrete Repair, Rehabilitation and Retrofitting III C R C Press LLC. 2012, pp. 521–524.

Please cite this article as: I. Viejo et al., Numerical modelling of porous cement-based materials by superabsorbent polymers, Cement and Concrete Research (2016), http://dx.doi.org/10.1016/j.cemconres.2016.07.018